AD-A191 730 EFFECT OF UNIAXIAL STRESS ON THE RAMAN SPECTRA OF GRAPHITE FIBERS(U) MASSACHUSETTS INST OF TECH CAMBRIDGE H SAKATA ET AL. 30 OCT 87 AFOSR-TR-88-0226 1/1

UNCLASSIFIED F49629-85-C-0147 F/G 11/2.1 NL

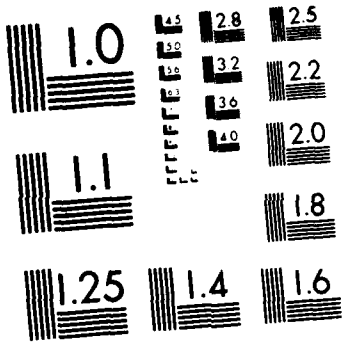

SECURITY CLASSIFICATION

AD-A191 730

TION PAGE

DTIC FILE COPY

(2)

1a. REPORT SECURITY CLASSIFICATION: Unclassifi	1b. RESTRICTIVE MARKINGS
2a. SECURITY CLASSIFICATION AUTHORITY	3. DISTRIBUTION/AVAILABILITY OF REPORT: Distribution Unlimited
2b. DECLASSIFICATION/DOWNGRADING SCHEDULE	
4. PERFORMING ORGANIZATION REPORT NUMBER(S)	5. MONITORING ORGANIZATION REPORT NUMBER(S): AFOSR-TR- 88-0226
6a. NAME OF PERFORMING ORGANIZATION: Massachusetts Institute of Technology	6b. OFFICE SYMBOL (If applicable):
6c. ADDRESS (City, State and ZIP Code): Rm. 13-3005, MIT, 77 Massachusetts Avenue, Cambridge, MA 02139	7a. NAME OF MONITORING ORGANIZATION: AFOSR/NE NC
	7b. ADDRESS (City, State and ZIP Code): Building 410, Bolling Air Force Base, DC 20332-6448
8a. NAME OF FUNDING/SPONSORING ORGANIZATION: AFOSR	8b. OFFICE SYMBOL (If applicable): NE NC
	9. PROCUREMENT INSTRUMENT IDENTIFICATION NUMBER: F49629-85-C-0147
8c. ADDRESS (City, State and ZIP Code): AFOSR/NE ATTN: Dr. Don Ulrich, Bolling AFB, DC 20332-6448	10. SOURCE OF FUNDING NOS.

PROGRAM ELEMENT NO.	PROJECT NO.	TASK NO.	WORK UNIT NO.
61102F	2303	A3	

11. TITLE (Include Security Classification): Effect of Uniaxial Stress on the Raman Spectra of Graphite Fibers

12. PERSONAL AUTHOR(S): H. Sakata, G.Dresselhaus, M.S.Dresselhaus, M.Endo

13a. TYPE OF REPORT	13b. TIME COVERED	14. DATE OF REPORT (Yr., Mo., Day)	15. PAGE COUNT
Reprint	FROM 9-1-86 TO 8-31-87	October 30, 1987	15

16. SUPPLEMENTARY NOTATION

17. COSATI CODES			18. SUBJECT TERMS (Continue on reverse if necessary and identify by block number)
FIELD	GROUP	SUB. GR.	Effect of Uniaxial Stress on Raman Spectra of Carbon Fibers, Raman microprobe spectroscopy of single carbon fibers

19. ABSTRACT (Continue on reverse if necessary and identify by block number)

Measurements of the effect of uniaxial stress on the frequency of the zone center optical phonons in heat-treated benzene-derived graphite fibers have been performed using first-order Raman scattering. Application of uniaxial stress along the fiber axis was found to cause polarization-dependent splittings and shifts of the Raman peaks of the zone center doubly degenerate optical phonons. From these observed splittings and shifts, experimental values for the phenomenological coefficients which describe the changes in the elastic constant of these phonons with strain were determined. It is concluded that Raman spectroscopy can be used to characterize the local stress or strain conditions of graphite fibers nondestructively.

(Raymondi)

20. DISTRIBUTION/AVAILABILITY OF ABSTRACT	21. ABSTRACT SECURITY CLASSIFICATION
UNCLASSIFIED/UNLIMITED ☒ SAME AS RPT. ☐ OTIC USERS ☐	Unclassified

22a. NAME OF RESPONSIBLE INDIVIDUAL	22b. TELEPHONE NUMBER (Include Area Code)	22c. OFFICE SYMBOL
Dr. Don Ulrich	(202)767-4963	NE NC

DD FORM 1473, 83 APR EDITION OF 1 JAN 73 IS OBSOLETE.

DTIC ELECTED MAR 07 1988 S D

EFFECT OF UNIAXIAL STRESS ON THE RAMAN SPECTRA OF GRAPHITE FIBERS

H. Sakata†, G. Dresselhaus and M.S. Dresselhaus
Massachusetts Institute of Technology, Cambridge, MA 02139
M. Endo
Shinshu University, Nagano–shi 380, Japan

Abstract

Measurements of the effect of uniaxial stress on the frequency of the $\vec{k} \approx 0$ optical phonons in heat–treated benzene–derived graphite fibers using first–order Raman scattering have been performed. Application of uniaxial stress along the fiber axis is found to cause polarization–dependent splittings and shifts of the Raman peaks of the $\vec{k} \approx 0$ doubly degenerate optical phonons. From these observed splittings and shifts, experimental values for the phenomenological coefficients which describe the changes in the elastic constant of these phonons with strain are determined. It is concluded that Raman spectroscopy can be used to characterize the local stress or strain conditions of graphite fibers nondestructively.

Introduction

Laser Raman spectroscopy is a powerful nondestructive technique for monitoring the local stress variations near the surface of materials. The Raman microprobe used in this experiment provides $\sim 2\mu$m spatial resolution within the optical skin depth. This spatial resolution is to be contrasted with more conventional techniques such as x–ray analysis which typically have a spatial resolution of $\sim$ 1mm. Stress measurements in semiconductors such as Si[1], Ge[2] and GaAs[2] by Raman spectroscopy have been previously reported. Of particular interest for Raman spectroscopic studies of graphite is the anisotropy in the stress and strain parallel and perpendicular to the basal planes, so that polarization studies provide unique information on the elastic properties.

Graphite fibers are currently of interest to materials applications requiring high strength to weight ratio. However, no stress measurements in graphite fibers by Raman spectroscopy have been reported, though Raman measurements of the in–plane optical lattice mode have been shown to provide a sensitive method for the characterization of the structural perfection of carbon[3] and carbon fibers[4] [5]. Since the benzene–derived graphite fibers[6] are typically between 10 and 20μm in diameter, Raman spectroscopy can be used to examine the stress variation within the optical skin depth ($\sim$ 600Å for light scattering at 4880Å).

In this work, heat–treated benzene–derived graphite fibers are characterized by Raman spectroscopy as a function of applied uniaxial tensile stress. In the absence

†Permanent address: Mechanical Engineering Research Laboratory, Hitachi Ltd., Tsuchiura–shi, Ibaraki–ken 300, Japan

of uniaxial stress, the first–order Stokes Raman spectrum of graphite fibers exhibits a single peak which corresponds to the $\vec{k} \approx 0$ vibrations of the doubly degenerate optical phonons (E_{2g2}). The application of uniaxial stress causes polarization–dependent splittings and shifts which are observed to be linear in the applied stress in consequence of the change of the elastic constants with strain. From these observed splittings and shifts, experimental values for the phenomenological coefficients A and B which describe the changes in the elastic constant of the $\vec{k} \approx 0$ optical phonons with strain are determined.

Experimental Procedure

The carbon fibers used in the present investigation were prepared on a substrate by pyrolyzing a mixture of benzene and hydrogen at a temperature of $\sim$ 1100°C. After the fiber growth, graphitization of the fibers is accomplished by heat treatment at a temperature of 2900°C using a carbon–resistance furnace in a high–purity argon atmosphere. The resulting fibers consist of faceted concentric graphite layers around the fiber axis, such as the annular rings of a tree [6]. The fiber diameter used in this work was 7.6μm and the fiber length was 15 mm. As shown in Fig. 1, single fibers were bonded to the sample stage of the Raman microprobe at one end and to a nylon string which was connected to a pan containing weights at the other end. Uniaxial tensile stress was applied to the fibers by putting weights on the pan and thus the stress direction was coincident with the fiber axis.

The Raman scattering measurements were made at room temperature in the backscattering configuration using a Raman microprobe [7] with 488 nm Ar^+ laser excitation, a 40X objective lens (about 1μm spot size) and a diode array detector. The Raman spectra were taken for polarizations such that the electric vectors of the incident beam were either parallel or perpendicular to the stress direction of the fibers. Spectra were also taken for more than 8 points at random along the fiber axis at each stress level. The values of the peak position and half–width in the Raman spectra were determined by a Lorentzian fit to the experimental points.

Experimental Results

The doubly degenerate Raman mode at about 1580cm^{-1} which corresponds to the Raman–allowed E_{2g2} mode in HOPG was used for the Raman characterization. The disorder–induced line at about 1360cm^{-1} could barely be detected in the Raman spectra of the fibers used, indicating a nearly complete graphitization of the fibers and a nearly full establishment of three–dimensional graphite ordering[5].

Figure 2 shows typical Raman spectra of the fibers for the uniaxial tensile stress σ = 0 and 430 MPa. The stress σ is applied along the fiber axis, while the electric vector $\vec{E}$ of the incident beam is polarized either parallel or perpendicular to the stress direction, that is, $\vec{\sigma} \| \vec{E}$ and $\vec{\sigma} \perp \vec{E}$, respectively. For the fiber batch used in these experiments, the Raman shift of the peak in the absence of stress occurs at

$\omega_0 = 1583.2\text{cm}^{-1}$ and its half-width Γ_0 at half maximum intensity is 10.3 cm^{-1}. From Fig. 2, it can be seen that the application of uniaxial stress causes the Raman shift for the peak to split into two components which are observed for the two polarizations.

Figure 3 shows a plot of the Raman shift for the peak near 1580 cm^{-1} as a function of the uniaxial tensile stress σ. Since spectra were taken for more than 8 points at random along the fiber axis at each stress level, mean values and variation bars are shown in Fig. 3. The Raman shift of HOPG which was obtained in this experiment is also presented in this figure as a reference and it can be seen that the Raman shift of the fibers in the absence of stress is within 1 cm^{-1} of that of HOPG (ω = 1583.6 cm^{-1}). From our data in Fig. 3, it follows that the Raman shift decreases linearly with increasing σ in both cases ($\vec{\sigma}\|\vec{E}$ and $\vec{\sigma}\perp\vec{E}$) and the decrease in the case of $\vec{\sigma}\|\vec{E}$ is about 3.5 times faster than that of $\vec{\sigma}\perp\vec{E}$. The different behavior for the two polarizations corresponds to the splitting of the double degeneracy of the E_{2g_2} mode under uniaxial stress.

The variation in the half-width Γ at half maximum intensity of the 1580cm^{-1} lines as a function of σ for the two polarization directions is shown in Fig. 4. The half-width Γ_0 of the fibers in the absence of stress is about 10% larger than that of HOPG (Γ = 9.1 cm^{-1}). From Fig. 4, it can be seen that the half-width Γ increases linearly with increasing σ for both polarizations and the increase in the case of $\vec{\sigma}\|\vec{E}$ is about 3 times faster than that of $\vec{\sigma}\perp\vec{E}$. These half-width variations correspond to the inhomogeneous variation of the local stress or strain distribution.

Figure 5 shows a plot of the shift $\Delta\omega = \omega_0 - \omega_\sigma$, where ω_0 and ω_σ are the Raman shifts in the absence and presence of stress, respectively, as a function of σ. The data for diamond ($\vec{\sigma}\|[100], \vec{\sigma}\perp\vec{E}$)[8] and semiconducting materials such as Si[1], Ge[2] and GaAs[3] ($\vec{\sigma}\|[111], \vec{\sigma}\|\vec{E}$) are also presented in Fig. 5. From Fig. 5, it follows that $\Delta\omega$ for the fibers increases linearly with increasing σ for both polarizations and the increase of $\Delta\omega$ in the case of $\vec{\sigma}\|\vec{E}$ is about 3.5 times larger than that of $\vec{\sigma}\perp\vec{E}$. Thus the stress σ is related to $\Delta\omega$ by the following equations:

$$\sigma(MPa) = 168 \cdot \Delta\omega(cm^{-1}); \quad \sigma\|E \tag{1}$$

$$\sigma(MPa) = 588 \cdot \Delta\omega(cm^{-1}); \quad \sigma\perp E \tag{2}$$

These experimental measurements should be useful in engineering applications since the local stress can be estimated nondestructively by measurement of $\Delta\omega$. It can also be seen that the increase of $\Delta\omega$ for the benzene-derived graphite fibers is comparable to that for other materials shown in Fig. 5. We have been unable to obtain this measurement on crystalline graphite.

The relationship between $\Delta\omega$ and the strain ε which is calculated from the elastic modulus and the applied stress is shown in Fig. 6, where it is found that the strain dependence of $\Delta\omega$ for the graphite fibers is somewhat larger but comparable to that for typical semiconducting materials.

From this Raman scattering study of the characterization of heat-treated benzene derived graphite fibers under stress, it is concluded that Raman spectroscopy can be

A-1

used to provide complementary information on the local stress conditions of these fibers.

Theoretical Considerations

1 Stress–Strain Relations for Graphite Fibers

For hexagonal crystals, symmetry reduces the generalization of Hooke's law which relates an arbitrary stress to an arbitrary strain as follows

$$\begin{bmatrix} \epsilon_{xx} \\ \epsilon_{yy} \\ \epsilon_{zz} \\ \epsilon_{yz} \\ \epsilon_{zx} \\ \epsilon_{xy} \end{bmatrix} = \begin{bmatrix} S_{11} & S_{12} & S_{13} & 0 & 0 & 0 \\ S_{12} & S_{11} & S_{13} & 0 & 0 & 0 \\ S_{13} & S_{13} & S_{33} & 0 & 0 & 0 \\ 0 & 0 & 0 & S_{44} & 0 & 0 \\ 0 & 0 & 0 & 0 & S_{44} & 0 \\ 0 & 0 & 0 & 0 & 0 & 2(S_{11}-S_{12}) \end{bmatrix} \begin{bmatrix} \sigma_{xx} \\ \sigma_{yy} \\ \sigma_{zz} \\ \sigma_{yz} \\ \sigma_{zx} \\ \sigma_{xy} \end{bmatrix}. \tag{3}$$

The carbon fibers used in this experiment exhibit a unique structural morphology, since the carbon was deposited in a cylindrically symmetric fashion leading to a smooth uniform lamellar deposit in which the graphitic basal planes had a high degree of preferred orientation, lying nearly parallel to the fiber axis[6]. Hence, taking the coordinate system shown in Figure 7, for a uniaxial stress, σ, applied along the fiber axis,

$$\sigma_{xx} = \sigma \tag{4}$$

$$\sigma_{yy} = \sigma_{zz} = \sigma_{yz} = \sigma_{zx} = \sigma_{xy} = 0 \tag{5}$$

Also, for a uniaxial stress σ there are no shear components of strain, so

$$\epsilon_{yz} = \epsilon_{zx} = \epsilon_{xy} = 0 \tag{6}$$

Therefore, the stress–strain relations for graphite fibers are

$$\begin{aligned} \epsilon_{xx} &= S_{11}\sigma \\ \epsilon_{yy} &= S_{12}\sigma \\ \epsilon_{zz} &= S_{13}\sigma \end{aligned} \tag{7}$$

2 Strain-Dependent Raman Frequency in Graphite

In the presence of strain the dynamical equations which describe phonon modes in the solid have the form[1],[2],[8]

$$\bar{m}\ddot{u}_i = -\sum_j K_{ij}u_j \tag{8}$$

$$= -(K_{ii}^0 u_i + \sum_{jkl} \frac{\partial K_{ij}}{\partial \epsilon_{kl}}\epsilon_{kl}u_j) \tag{9}$$

where u_i is the i^{th} component of the relative displacement of the two atoms in the unit cell, $\bar{m}$ is the reduced mass of the two atoms, and $K_{ii}^0 = \bar{m}\omega_0^2$ is the effective spring constant of the phonon modes in the absence of strain. The double–dotted quantities indicate second derivatives. The quantity

$$\frac{\partial K_{ij}}{\partial \epsilon_{kl}}\epsilon_{kl} = K'_{ijkl}\epsilon_{kl} = K'_{ijlk}\epsilon_{lk} \tag{10}$$

is the change in the spring constant due to the applied strain ϵ_{kl}; i, j, k and l denote crystallographic axes.

From Eq. 9 the phonon frequencies for the strained lattice can be deduced. For pristine graphite with 4 atoms/unit cell a 12 × 12 secular determinant is obtained for the 3 acoustic and 9 optical modes. The hexagonal symmetry of the lattice results in a factorization of the secular determinant at $\vec{k} = 0$ and the result for the Raman active E_{2g2} mode is given by

$$\begin{vmatrix} A(\epsilon_{xx} + \epsilon_{yy}) - \lambda & B(\epsilon_{xx} - \epsilon_{yy} + 2i\epsilon_{xy}) \\ B(\epsilon_{xx} - \epsilon_{yy} - 2i\epsilon_{xy}) & A(\epsilon_{xx} + \epsilon_{yy}) - \lambda \end{vmatrix} = 0 \tag{11}$$

where

$$\lambda = \omega_\sigma^2 - \omega_0^2. \tag{12}$$

The parameter ω_σ is the strain–dependent Raman frequency and ω_0 is the frequency in the absence of strain. The above can be approximated as

$$\omega_\sigma \approx \omega_0 + \frac{\lambda}{2\omega_0}. \tag{13}$$

Since the shear components of strain vanish, the secular equation reduces to

$$\begin{vmatrix} A(\epsilon_{xx} + \epsilon_{yy}) - \lambda & B(\epsilon_{xx} - \epsilon_{yy}) \\ B(\epsilon_{xx} - \epsilon_{yy}) & A(\epsilon_{xx} + \epsilon_{yy}) - \lambda \end{vmatrix} = 0. \tag{14}$$

Hence there are two solutions:

$$\begin{aligned} \lambda_1 &= (A + B)\epsilon_{xx} + (A - B)\epsilon_{yy} \\ \lambda_2 &= (A - B)\epsilon_{xx} + (A + B)\epsilon_{yy}. \end{aligned} \tag{15}$$

Substituting the stress–strain relations (Eq. 7) into Eq. 15, the stress–dependent Raman frequencies become

$$\begin{aligned} \omega_{\sigma 1} &= \omega_0 + \frac{\sigma}{2\omega_0}\{(A + B)S_{11} + (A - B)S_{12}\} \\ \omega_{\sigma 2} &= \omega_0 + \frac{\sigma}{2\omega_0}\{(A - B)S_{11} + (A + B)S_{12}\}. \end{aligned} \tag{16}$$

The shifts in the Raman frequency due to strain, $\Delta\omega_1$ and $\Delta\omega_2$, are

$$\begin{aligned} \Delta\omega_1 &= \omega_0 - \omega_{\sigma 1} = -\frac{\sigma}{2\omega_0}\{(A + B)S_{11} + (A - B)S_{12}\} \\ \Delta\omega_2 &= \omega_0 - \omega_{\sigma 2} = -\frac{\sigma}{2\omega_0}\{(A - B)S_{11} + (A + B)S_{12}\}. \end{aligned} \tag{17}$$

Using the values for the elastic compliance constants in graphite, which have been determined[9] and the experimental data for the relationship between the applied uniaxial stress σ and the shift $\Delta\omega_1$ or $\Delta\omega_2$, the phenomenological coefficients A and B which describe the changes in the elastic constant of the $\vec{k} = 0$ optical phonons with strain are determined:

$$\begin{aligned} \mathrm{A} &= -1.44 \times 10^{7}\mathrm{cm}^{-2} \\ \mathrm{B} &= \pm 5.80 \times 10^{6}\mathrm{cm}^{-2} \end{aligned} \tag{18}$$

From the above, it is clear that the Raman effect can be used to characterize the strain induced in a carbon fiber which is subjected to an unknown stress load, σ, either externally or internally. If polarized light ($\vec{E} \parallel \vec{\sigma}$ and $\vec{E} \perp \vec{\sigma}$) is used for the Raman characterization, the shift of the frequency of the E_{2g2} Raman active mode will give information on the magnitude of the stress (or the strain) and its homogeneity along the fiber axis on a $\pm 2\mu$m resolution scale, using Eqs. 17 and 18. From the linewidth, additional information is provided on the uniformity of the local strains. If unpolarized light is used, the shift of the E_{2g2} Raman-active mode $\Delta\omega$ will be a linear combination of $\Delta\omega_1$ and $\Delta\omega_2$, which for completely random polarization becomes $\Delta\omega = (\Delta\omega_1 + \Delta\omega_2)/2$. In this case, the linewidth will mostly reflect the superposition of the contributions of the two polarization contributions which may not be well resolved.

Conclusions

1. Raman spectroscopy can be used to provide complementary information on the local stress conditions of graphite fibers. The local stress can be estimated nondestructively by measurement of $\Delta\omega$.

2. The stress dependence of the first-order Raman spectra associated with the $\vec{k} \approx 0$ optical phonons in graphite fibers has enabled us to determine values for the phenomenological coefficients which describe the changes in the spring constant of these optical phonons with strain.

Acknowledgments

We wish to thank Mr. P. Berthier for assistance with the heat treatment, and Mr. T. Kono for assistance with the measurements. This work was supported by AFOSR Contract #F49620-85-C-0147.

References

[1] E. Anastassaki, A. Pinczuk, E. Burstein, F. Pollak, and M. Cardona. *Solid State Commun.*, **8**, 133, (1970).

[2] F. Cerdeira, C. Buchenauer, F. Pollak, and M. Cardona. *Phys. Rev.*, **B5**, 580, (1972).

[3] F. Tuinstra and J. Koenig. *J. Chem. Phys.*, **53**, 1126, (1970).

[4] P. Kwizera, A. Erbil, and M.S. Dresselhaus. *Carbon*, **19**, 144-146, (1981).

[5] T. Chieu, M. Dresselhaus, and M. Endo. *Phys. Rev.*, **B26**, 5867, (1982).

[6] T. Koyama, M. Endo, and Y. Onuma. *Jap. J. Appl. Phys.*, **11**, 445, (1972).

[7] L. McNeil, J. Steinbeck, L. Salamanca-Riba, and G. Dresselhaus. *Carbon*, **24**, 73, (1986).

[8] S. Ganesan, A. Maradudin, and J. Oitmaa. *Annals of Phys.*, **56**, 556, (1970).

[9] B. Kelly. *Physics of Graphite*, Applied Science Pub., 74, (1981).

Figure Captions

Figure 1: Schematic drawing of the experimental setup for Raman scattering.

Figure 2: Line shape of the optical phonon E_{2g2} of the fibers for the uniaxial stress $\sigma = 0$ and 430 MPa. The solid line is the best Lorentzian fit to the experimental points. The dashed line indicates the position of the Raman shift ω_0 in the absence of stress. The arrows indicate the positions of the Raman shift for the peak in the presence of stress. In the case of $\sigma = 430$MPa, the Raman shift of the peak occurs at $\omega = 1580.6$ and 1582.4 cm^{-1} and its HWHM linewidth Γ is 11.4 and 10.6 cm^{-1} for $\vec{\sigma} \| \vec{E}$ and $\vec{\sigma} \perp \vec{E}$, respectively.

Figure 3: Plot of the Raman shift for the peak near 1580cm^{-1} vs. the applied uniaxial tensile stress σ. The full and open circles indicate the mean values for the Raman shift of the peak for the graphite fibers for the two senses of polarization. The error bars are also given. For comparison the value for HOPG is included.

Figure 4: Plot of the half-width Γ for the peak near 1580cm^{-1} vs. the applied uniaxial tensile stress σ. The full and open circles indicate the mean values for the HWHM linewidth for the two senses of polarization. The error bars are also given. Also included is the value for HOPG.

Figure 5: Plot of $\Delta\omega = \omega_0 - \omega_\sigma$ vs. the applied uniaxial tensile stress σ for graphite fibers (G.F.) including the two senses of polarization of the light and the corresponding results for typical semiconductors. The full and open circles indicate the mean values for the $\Delta\omega$ measurements and the error bars are also given.

Figure 6: Plot of the experimental shift $\Delta\omega$ vs. the calculated strain ϵ, which is estimated from the elastic modulus for graphite (including both $\vec{\sigma} \| \vec{E}$ and $\vec{\sigma} \perp \vec{E}$ polarizations). For comparison, the corresponding results for Si, Ge and diamond are included.

Figure 7: Coordinate system for a crystallite in a graphite fiber. The x axis is taken parallel to the fiber axis and is coincident with the direction of the applied uniaxial tensile stress σ.

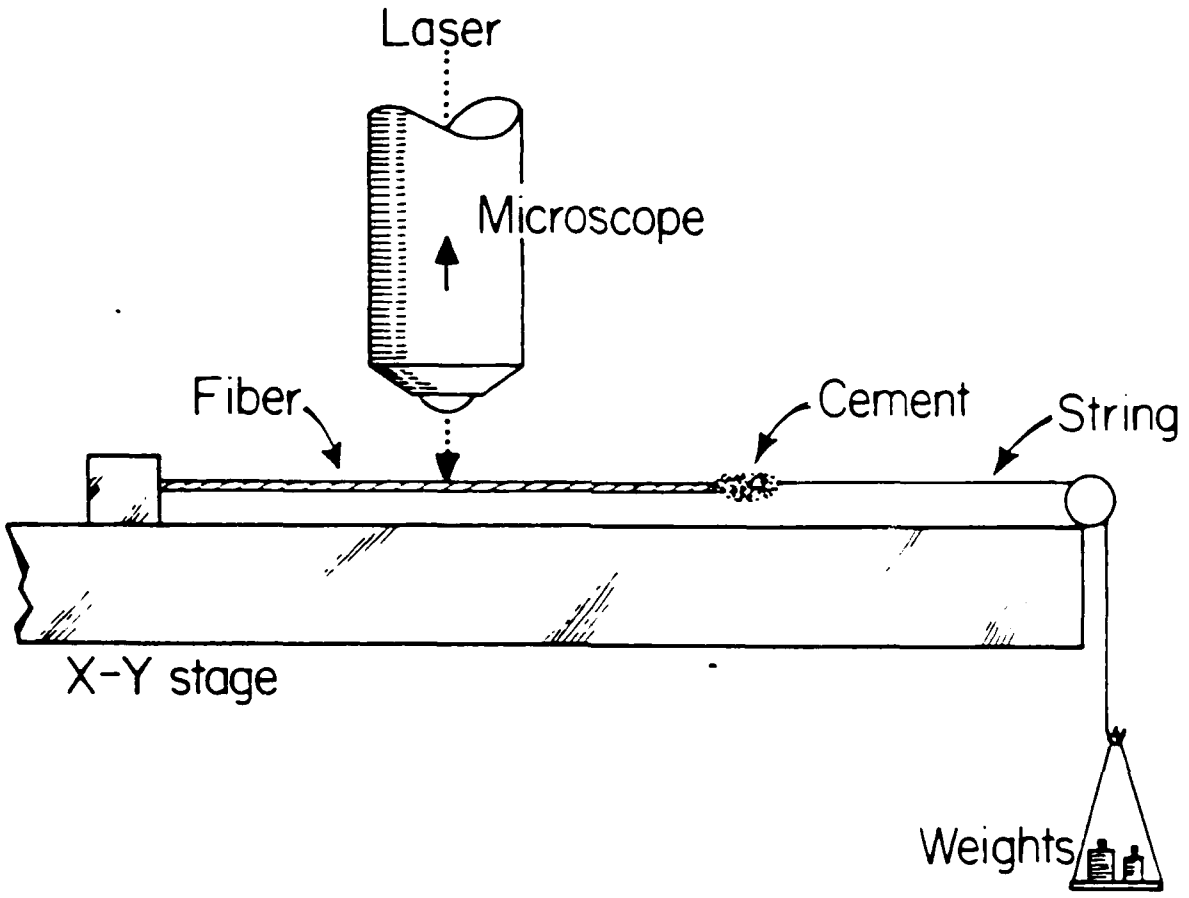
Laser
Microscope
Fiber
Cement
String
X-Y stage
Weights

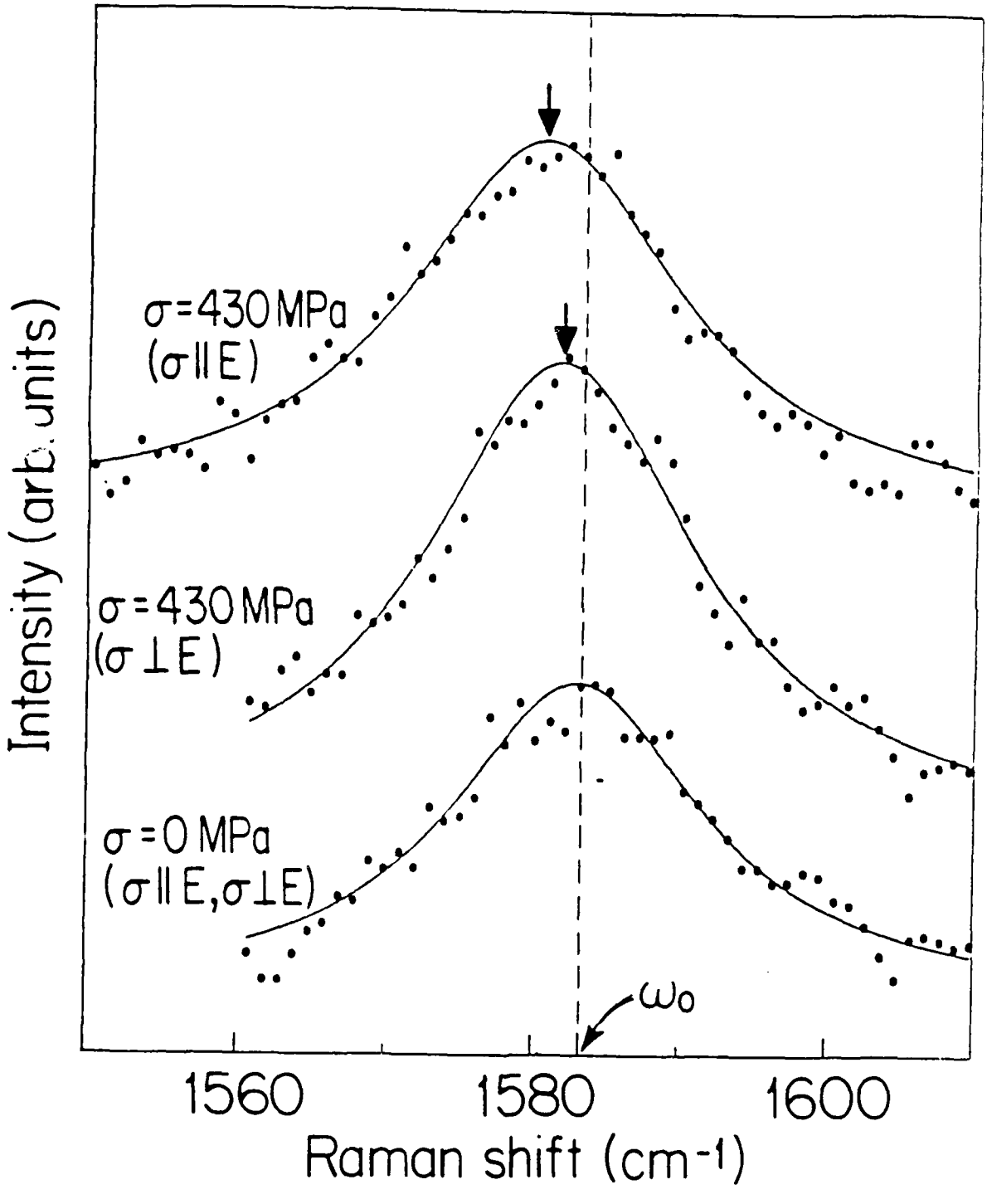
σ=430 MPa
(σ∥E)
σ=430 MPa
(σ⊥E)
σ=0 MPa
(σ∥E, σ⊥E)
ω0
Intensity (arb. units)
1560
1580
1600
Raman shift (cm-1)

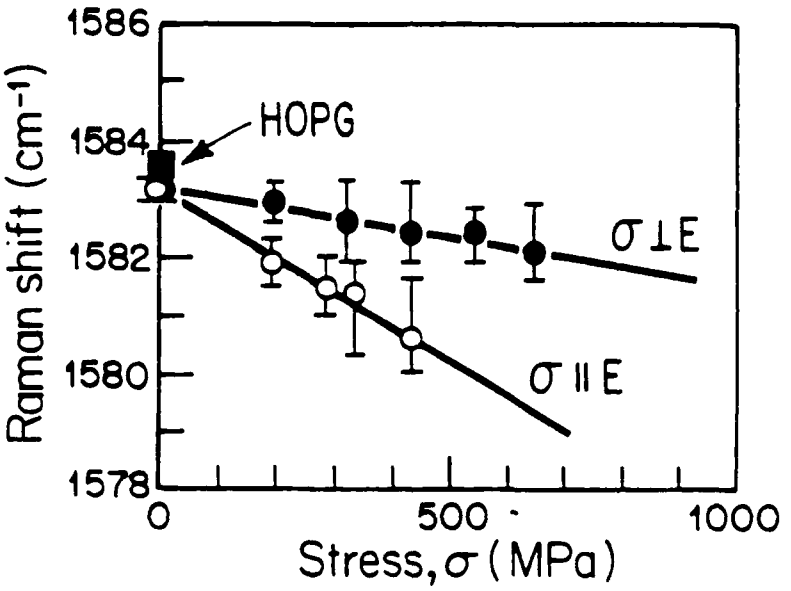
1586
1584
1582
1580
1578
HOPG
σ⊥E
σ∥E
Raman shift (cm-1)
0
500
1000
Stress, σ (MPa)

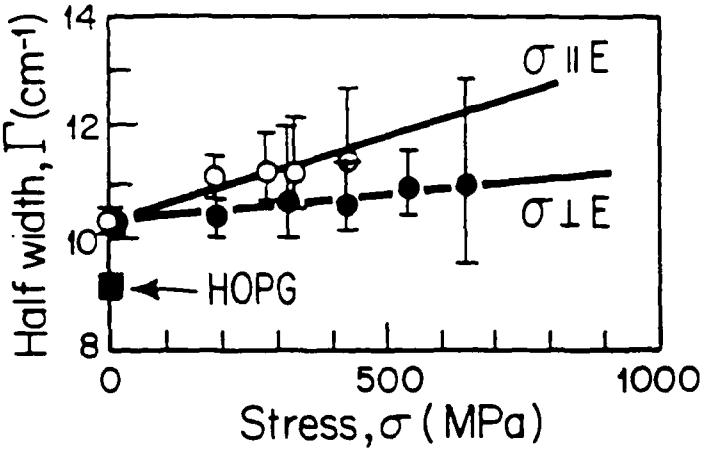
Half width, Γ(cm⁻¹)
14
12
10
8
σ ∥ E
σ ⊥ E
HOPG
0
500
1000
Stress, σ (MPa)

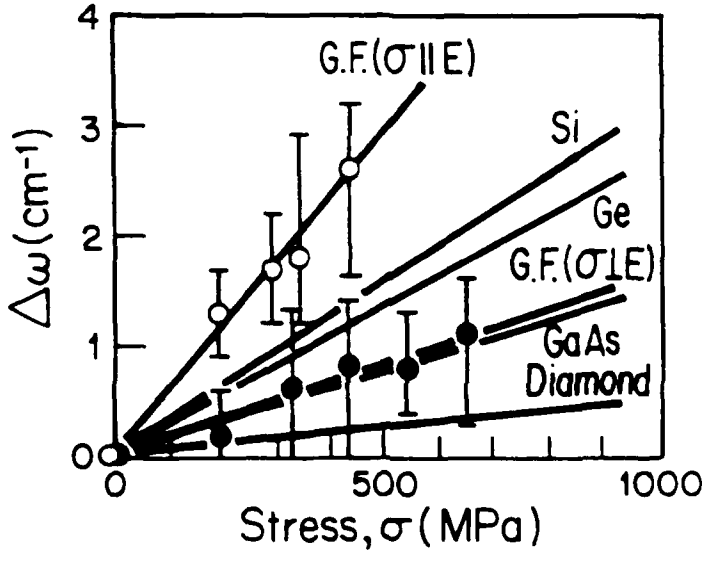
4
3
2
1
0
0
500
1000
Δω(cm⁻¹)
Stress, σ (MPa)
G.F.(σ ∥ E)
Si
Ge
G.F.(σ ⊥ E)
GaAs
Diamond

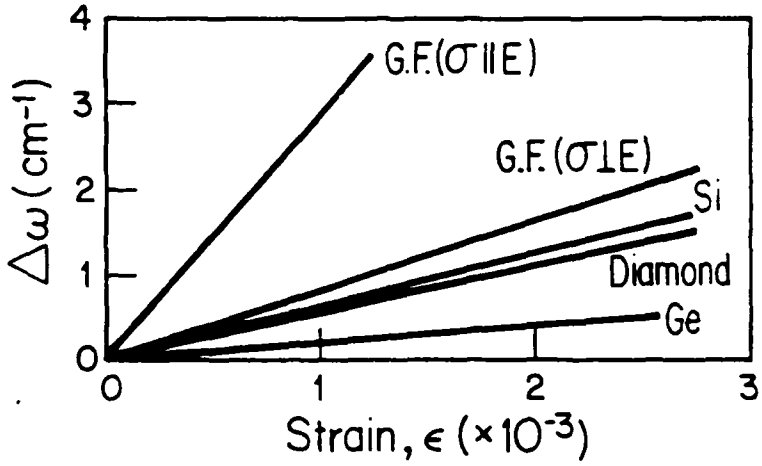
4
3
2
1
0
Δω (cm⁻¹)
G.F.(σ ∥ E)
G.F. (σ ⊥ E)
Si
Diamond
Ge
0
1
2
3
Strain, ϵ (×10⁻³)

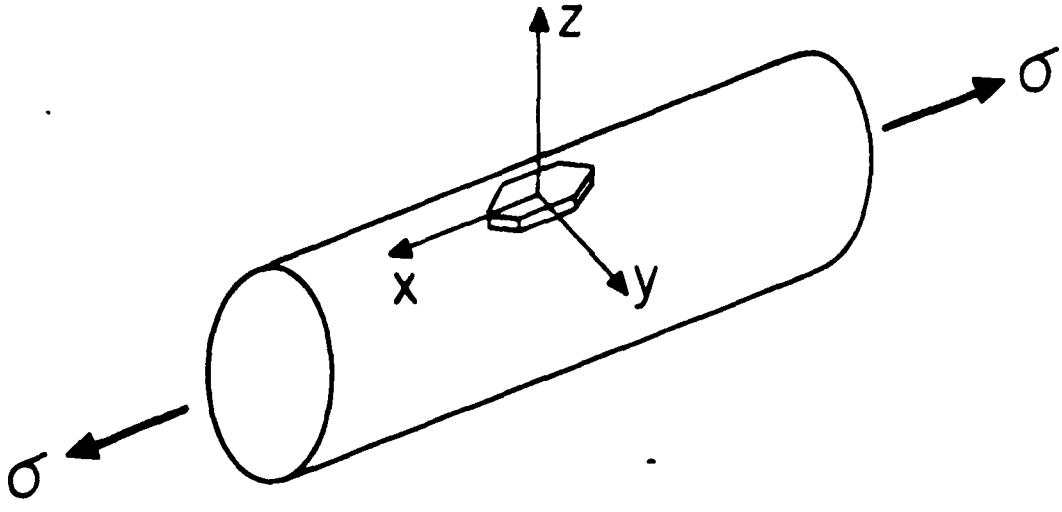
z
σ
x
y
σ

END

DATE

FILMED

5-88

DTIC